Supporting Information

Assembly of bacterial cell division protein FtsZ into dynamic biomolecular condensates

Miguel Ángel Robles-Ramos[1,3], Silvia Zorrilla[1,3]*, Carlos Alfonso[1], William Margolin[2], Germán Rivas[1]*, Begoña Monterroso[1]*

[1]Centro de Investigaciones Biológicas Margarita Salas, Consejo Superior de Investigaciones Científicas (CSIC). Madrid, Spain.

[2]Department of Microbiology and Molecular Genetics, McGovern Medical School, University of Texas. Houston, TX, USA.

[3]These authors contributed equally to this work.

*Corresponding authors: silvia@cib.csic.es (S.Z.); grivas@cib.csic.es (G.R.); monterroso@cib.csic.es (B.M.). Centro de Investigaciones Biológicas Margarita Salas, Consejo Superior de Investigaciones Científicas (CSIC). Ramiro de Maeztu, 9. 28040 Madrid, Spain. Tel. +34 918373112.

Table of contents **Page**

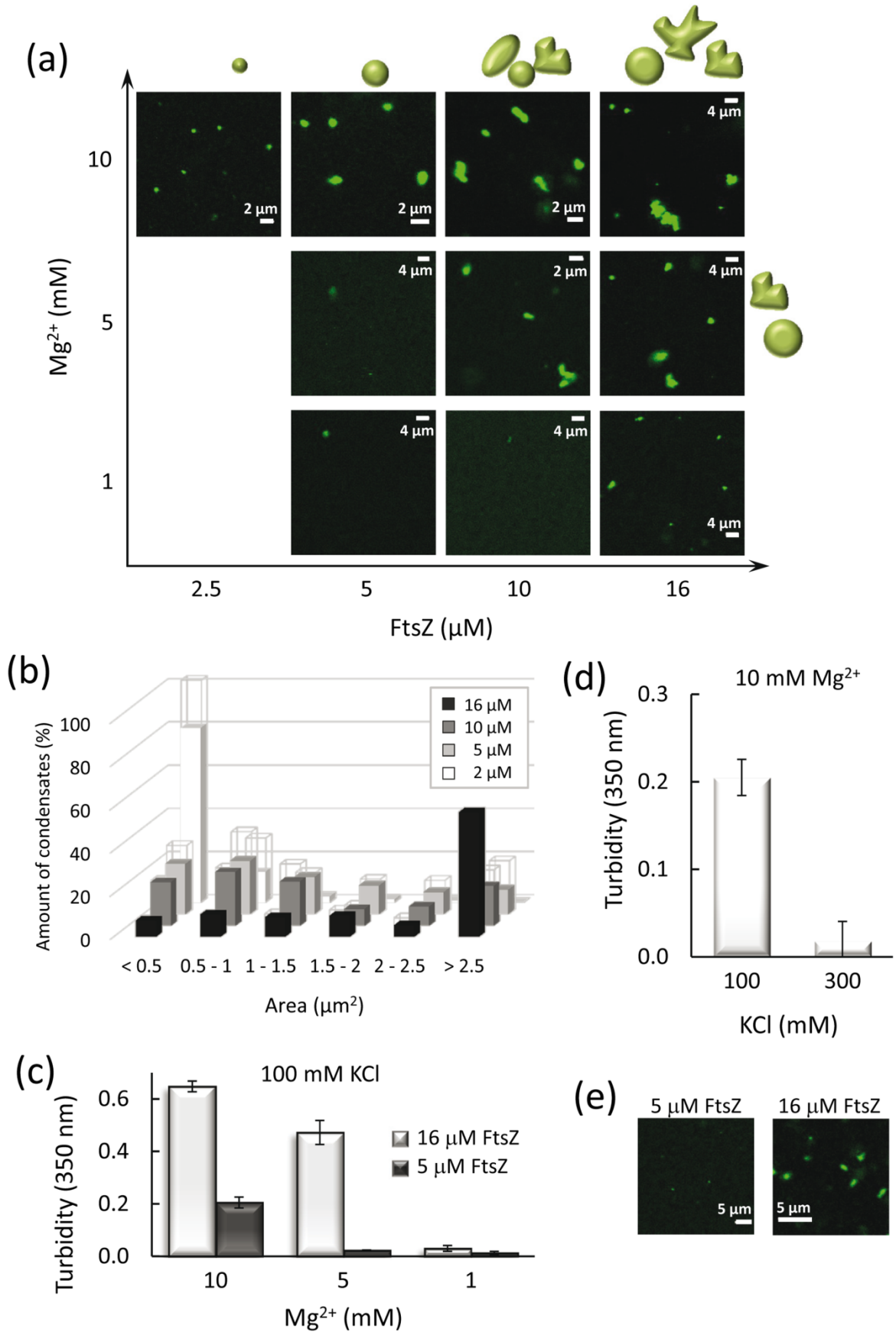
(a)
10
5
1
Mg2+ (mM)
2.5
5
10
16
FtsZ (µM)
2 µm
4 µm
(b)
Amount of condensates (%)
100
80
60
40
20
0
16 µM
10 µM
5 µM
2 µM
< 0.5
0.5 - 1
1 - 1.5
1.5 - 2
2 - 2.5
> 2.5
Area (µm2)
(c)
100 mM KCl
Turbidity (350 nm)
0.6
0.4
0.2
0.0
16 µM FtsZ
5 µM FtsZ
10
5
1
Mg2+ (mM)
(d)
10 mM Mg2+
Turbidity (350 nm)
0.3
0.2
0.1
0.0
100
300
KCl (mM)
(e)
5 µM FtsZ
16 µM FtsZ
5 µm

▲ **Supplementary Fig. S1.** Dependence of the formation of FtsZ arrangements with magnesium, protein and KCl concentration in dextran. (**a**) Representative confocal images of the structures formed by FtsZ, with FtsZ-Alexa 488 as a tracer, at the specified magnesium and protein concentrations in 100 mM KCl. (**b**) Size distribution of condensates, in working buffer, at various FtsZ concentrations (in ascending order, *n* = 124, 99, 80 and 106 particles). Errors, depicted as open sections of the bars, correspond to S.D. from 3 (2 and 5 μM FtsZ) or 2 (10 and 16 μM FtsZ) independent images. (**c**) Variation in the turbidity signal of FtsZ with magnesium at two FtsZ concentrations. (**d**) Variation in the turbidity signal of FtsZ (5 μM) with KCl concentration. Data in (c) and (d) are the average of at least 3 independent experiments ± S.D. (**e**) Structures formed by FtsZ with 300 mM KCl and 10 mM magnesium, at the specified FtsZ concentrations. Dextran was 200 g/l in all experiments.

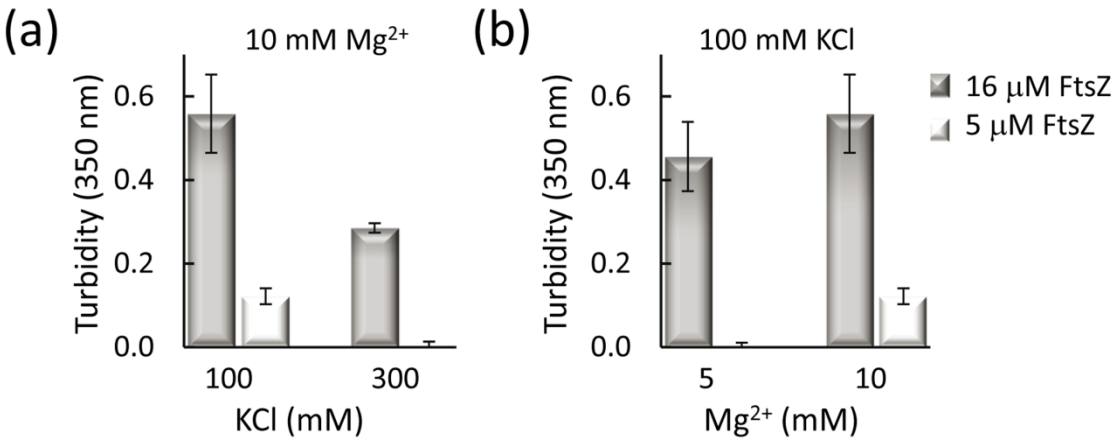

Supplementary Fig. S2. Formation of FtsZ condensates in Ficoll under different experimental conditions. Variation in the turbidity signal of FtsZ with KCl (**a**) and magnesium concentrations (**b**). Data are the average of at least 3 independent experiments ± S.D. In all experiments, Ficoll was 250 g/l. Note that signals correspond to all structures present in the solution, condensates and/or irregular arrangements depending on the case.

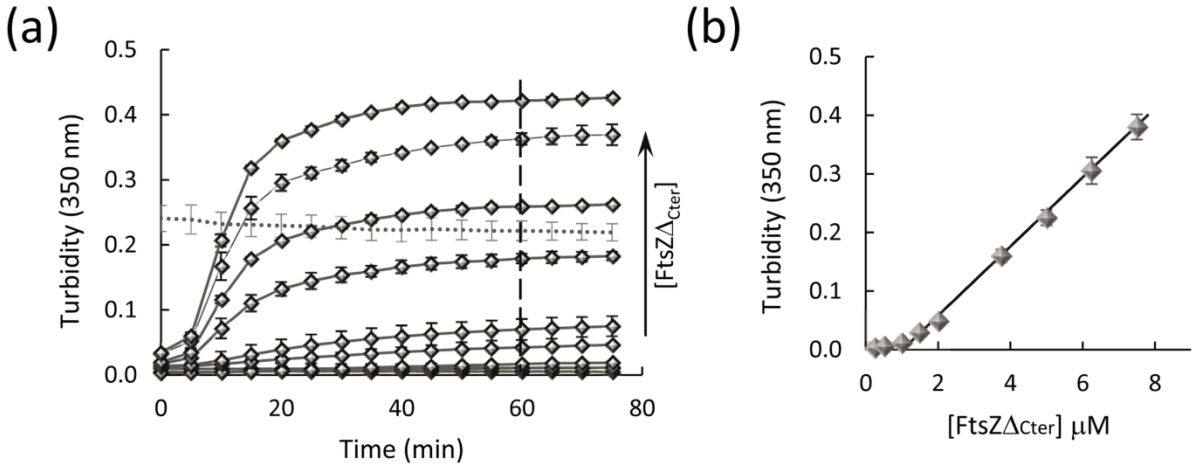

Supplementary Fig. S3. FtsZΔ_{Cter} forms condensates less efficiently. (**a**) Evolution with time of the turbidity signal of mutant FtsZ at different concentrations of the protein. From bottom to top: 0.1, 0.25, 0.5, 1, 1.5, 2, 3.8, 5, 6.3 and 7.5 μM. Four independent experiments were performed, from which the average of 2 (simultaneously measured) ± S.D. is shown as representative of the whole set. The dotted line corresponds to the turbidity signal of 5 μM wild-type FtsZ, averaged from 3 independent experiments ± S.D., shown as a reference. (**b**) Dependence of the turbidity signal of FtsZΔ_{Cter} on protein concentration. Symbols are data at equilibrium, average of 4 independent experiments ± S.D, extracted at the time point indicated in (a) with a dashed line. Solid line corresponds to a linear model fit to the data. All experiments were in working buffer with 200 g/l dextran.

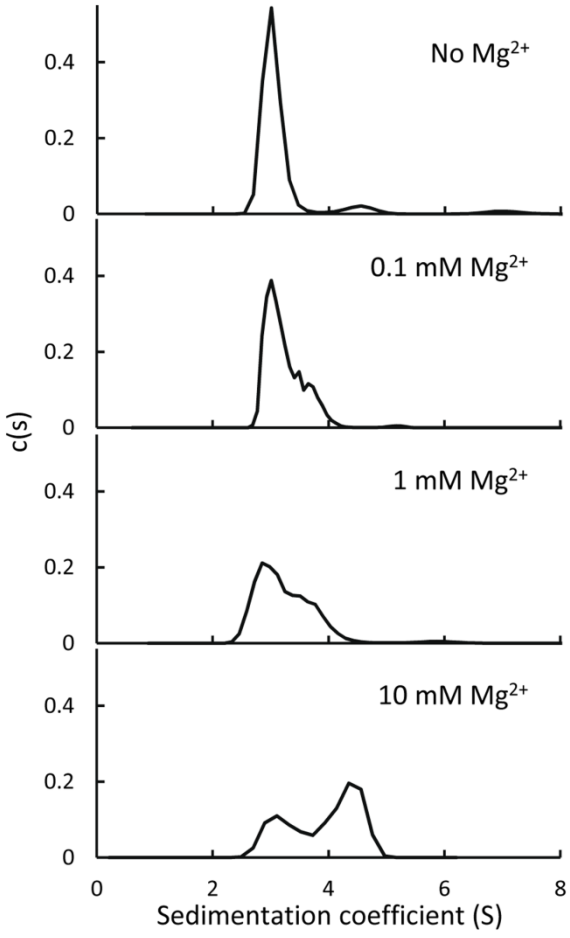

Supplementary Fig. S4. Effect of magnesium on the self-association of FtsZΔ_{Cter} as determined by analytical ultracentrifugation. Shown are sedimentation coefficient distributions of the mutant (15 μM) in 50 mM Tris-HCl pH 7.5, 300 mM KCl, with the specified magnesium concentrations.

Sedimentation velocity experiments of FtsZ mutant. Experiments were conducted in a XL-I analytical ultracentrifuge (Beckman-Coulter Inc.) equipped with both UV-VIS and Raleigh interference detection systems, using an An-50Ti rotor and 12 mm double sector centerpieces. Sedimentation profiles of samples containing $FtsZ\Delta_{Cter}$ centrifuged at 48000 rpm and 20 °C were recorded at 260 nm. Concentration of the mutant and experimental conditions are specified in the legend of the figure. Sedimentation coefficient distributions were calculated by least squares boundary modelling of sedimentation velocity data using the c(s) method with SEDFIT [1]. Experimental sedimentation coefficient values (s) were corrected to standard conditions using the program SEDNTERP [2] to obtain the corresponding standard s values ($s_{20,w}$).

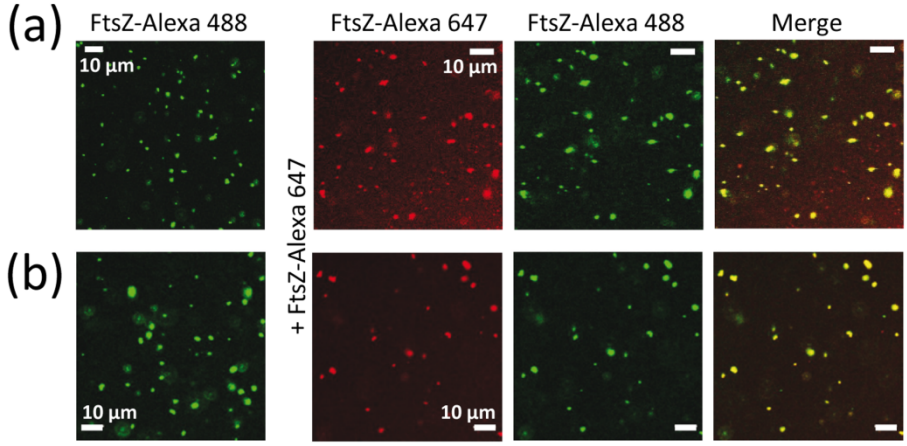

Supplementary Fig. S5. Representative confocal images showing the dynamism of FtsZ condensates under different experimental conditions. Initial and final states after addition of FtsZ-Alexa 647 into FtsZ condensates with FtsZ-Alexa 488 as a tracer (**a**) at time zero (after 30 min incubation) and (**b**) after 4h incubation. All experiments were with 5 µM FtsZ in working buffer with 200 g/l dextran.

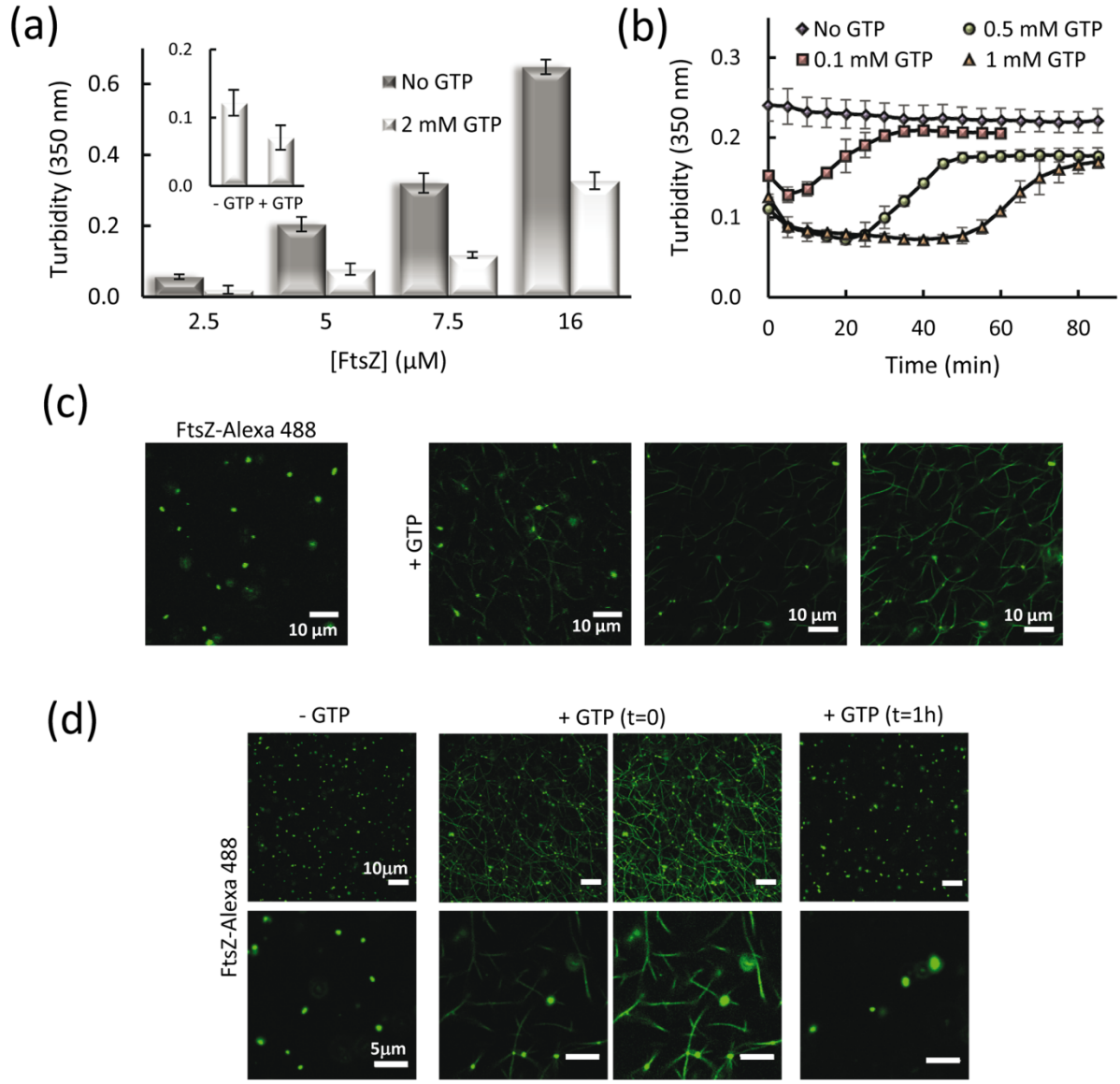

Supplementary Fig. S6. FtsZ within the condensates remains active for polymerization and interchange between both structures is reversible. (**a**) Effect of GTP addition on the turbidity signal of FtsZ in dextran at different concentrations of the protein. Inset shows the effect of 0.5 mM GTP addition on the turbidity signal of FtsZ in 250 g/l Ficoll. (**b**) Variation in the turbidity signal of FtsZ upon triggering polymerization by addition of the specified GTP concentrations. Evolution of the signal in the absence of GTP is shown for reference. Data in (a) and (b) are the average of at least 3 independent experiments ± S.D. The "no GTP" statement refers to samples where no GTP was added (*i.e.* FtsZ-GDP). (**c**) Representative confocal images of FtsZ condensates, incubated 4 h, before and after addition of GTP (0.5 mM). The image at the far right was obtained by enhancing the brightness (44%) of the one next to it (correction applied uniformly to the whole image, using Microsoft PowerPoint) to better appreciate the polymerization of FtsZ into filaments. (**d**) Confocal images showing the conversion of FtsZ condensates into GTP-triggered polymers and back. Immediately after addition of GTP (0.1 mM, t = 0), polymers are starting to be observed. For GTP and time zero, images within the same row are the identical field, with the images on the right obtained by enhancing the brightness (40%, top; 60%, bottom) of the ones on the left (correction applied uniformly to the whole image, using Microsoft PowerPoint) to better appreciate the polymerization of FtsZ. All experiments were in working buffer, with 200 g/l dextran except inset in (a), and 5 μM or the specified FtsZ concentrations.

Supplementary references

1. Schuck, P. (2000). Size-distribution analysis of macromolecules by sedimentation velocity ultracentrifugation and lamm equation modeling. *Biophys J* **78**, 1606-19.
2. Laue, T. M., B. D. Shah, T. M. Ridgeway, and S. L. Pelletier. (1992). Computer-aided interpretation of analytical sedimentation data for proteins. In *Analytical Ultracentrifugation in Biochemistry and Polymer Science* (S. E. Harding and A. J. Rowe, ed.). The Royal Society of Chemistry, Cambridge, UK.